Available online at www.sciencedirect.com
SCIENCE DIRECT®
Journal of Theoretical Biology 225 (2003) 171–183
Journal of Theoretical Biology
www.elsevier.com/locate/jtbi

Simultaneous analysis of prompt and delayed chlorophyll *a* fluorescence in leaves during the induction period of dark to light adaptation

V. Goltsev[a,*], I. Zaharieva[a,b], P. Lambrev[a,b], I. Yordanov[c], R. Strasser[d]

[a] *Department of Biophysics and Radiobiology, Faculty of Biology, St. Kliment Ohridski University of Sofia, 8, Dragan Tzankov Blvd., 1164, Sofia, Bulgaria*
[b] *Institute of Biophysics, Bulgarian Academy of Sciences, Bulgaria*
[c] *Institute of Plant Physiology, Bulgarian Academy of Sciences, Bulgaria*
[d] *Bioenergetics Laboratory, University of Geneva, CH-1254 Jussy, Genève, Switzerland*

Received 15 May 2002; received in revised form 24 March 2003; accepted 5 June 2003

Abstract

An attempt is made to reveal the relation between the induction curves of delayed fluorescence (DF) registered at 0.35–5.5 ms and the prompt chlorophyll fluorescence (PF). A simple formulation was proposed to link the ratio of the transient values of delayed and variable fluorescence with the redox state of the primary electron acceptor of Photosystem II—Q_A, and the thylakoid membrane energization. The term luminescence potential (U_L) was introduced, defined as the sum of the redox potential of Q_A and the transmembrane proton gradient. It was shown that U_L is proportional to the ratio of *DF* to the variable part of *PF*. The theoretical model was verified and demonstrated by analysing induction courses of *PF* and millisecond *DF*, simultaneously registered from leaves of barley—wild-type and the chlorophyll *b*-less mutant *chlorina f2*. A definitive correlation between *PF* and *DF* was established. If the luminescence changes are strictly due to U_L, the courses of *DF* and *PF* are reciprocal and the millisecond *DF* curve resembles the first derivative of the $PF(t)$ function.

Keywords: Delayed fluorescence; Variable chlorophyll fluorescence; Induction curves; Photosystem II; Barley *chlorina f2* mutant

1. Introduction

The ability of the chlorophyll molecule not only to absorb light and to carry out the primary photochemical reaction, but also to dissipate part of this energy as fluorescence, makes the fluorescence a very convenient probe for the state of the photosynthetic apparatus.

Luminescence methods based on registration of light emitted by Photosystem II (PS II), both of prompt and delayed chlorophyll fluorescence, are among the most perspective biophysical methods to evaluate the physiological state of the plant. Although light quanta are emitted by the same population of molecules (predominantly chlorophyll molecules of PS II antenna complexes) (Amesz and Van Gorkom, 1978), the two types of luminescence contain information about different fundamental processes of the photosynthetic apparatus (Vesselovskii and Veselova, 1990; Krause and Weis, 1991). The simultaneous registration and analysis of both luminescence types extends our knowledge and understanding about the current state of the photosynthetic sample.

The aim of the present study was to reveal the relation between the millisecond delayed and the prompt chlorophyll fluorescence during the induction period. The comparison is based on results from synchronized registration of induction curves of prompt fluorescence and delayed fluorescence decaying in the micro- and

Abbreviations: PF, prompt chlorophyll fluorescence; DF, delayed chlorophyll fluorescence; RC, reaction centre; PS I, Photosystem I; PS II, Photosystem II; F_0, initial (dark) fluorescence; F_v, variable fluorescence; F_p F_s F_t, fluorescence intensities at characteristic moments of induction; LHCI and LHCII, light-harvesting complexes of PS I and PS II; PQ, plastoquinone; U_L, luminescence potential.

*Corresponding author. Tel.: +26-662-23; fax: +268-566-41.
E-mail address: goltsev@biofac.uni-sofia.bg (V. Goltsev).

0022-5193/03/$ - see front matter © 2003 Elsevier Ltd. All rights reserved.
doi:10.1016/S0022-5193(03)00236-4

milliseconds time range. A simple equation was proposed linking both prompt and delayed fluorescence with the redox state of the PS II electron carriers. It allows us to relate the *DF* induction curves with the light-driven processes that take place during the transition of the photosynthetic sample from dark- to light-adapted state. An example is presented of applying this model to characterize photosynthetic samples with different PS II antenna size.

2. Theoretical background

The changes in chlorophyll fluorescence after illumination of dark-adapted plants were first observed by Kautsky and Hirsch (1931) and delayed light emission by plants was discovered by Strehler and Arnold (1951). During the last two decades, research was focused mainly on the prompt (variable) chlorophyll fluorescence—studying the mechanisms of its formation and applying it to fundamental and practical photosynthesis studies (Krause and Weis, 1991; Govindjee, 1995; Strasser et al., 1995). Because of the technical complexity of delayed fluorescence registration and investigation, the knowledge about its mechanisms is far behind.

3. Origin of the delayed and variable chlorophyll fluorescence

According to the radical pair hypothesis, *DF* originates from recombination of P^+I^- and occurs with a 2–4 ns lifetime (Jursinic, 1986). For a light quantum to be emitted, a chain of successive photophysical, photochemical and chemical reactions must be realized:

$$PI \xrightarrow{h\nu} P^*I \rightarrow P^+I^- \rightarrow P^*I.$$

The chain of redox reactions within PS II controls the variable and delayed chlorophyll fluorescence:

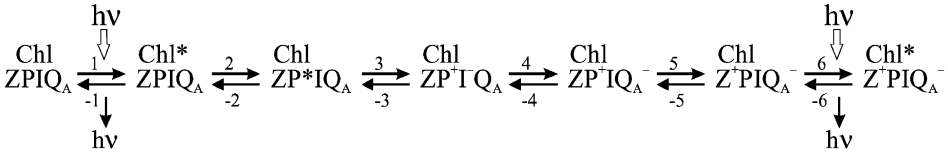

where Chl represents the antenna chlorophylls, P is the photochemically active pigment of the PS II reaction centre chlorophyll (P_{680}), I and Q_A are the primary and secondary electron acceptors, respectively, and Z is the secondary electron donor (Y_Z).

There are two types of emission from PS II: (i) *PF* with intensity depending on the momentary redox state of the RC acceptors and the donor (Butler, 1977; Shinkarev and Govindjee, 1993). *PF* includes: F_0—initial fluorescence that is emitted before the excitation energy has reached the reaction centre (includes reactions 1 and –1 on the diagram) and F_v—variable fluorescence—excitation energy has reached a closed reaction centre (the state after reaction 5), which cannot stabilize separated charges and the energy is radiated back (reactions 6 and –6). (ii) *DF*, which is radiated as a result of electron transfer to Q_A (reactions 1–5), Q_B or further in the chain and then backwards leading to charge recombination and secondary excitation of the reaction centre (back reactions –5 to –1).

A more detailed tentative scheme combining the biochemical species with the *PF* and *DF* signals was presented recently (Stirbet and Strasser, 2001).

4. Dark decay of delayed fluorescence

Since all redox reactions in the photosynthetic electron transport chain are theoretically reversible, there is certain probability that the electron is transferred back at each particular step in the donor or acceptor side. This is one of the reasons of the existence of many *DF* kinetic components. They differ by their characteristic decay lifetime as well as by their amplitude. The reactions corresponding to these components may have different activation energies which allows them to occur at specific temperatures as thermoluminescence bands (deVault et al., 1983; Vass and Govindjee, 1996). The total relaxation kinetics of *DF* is defined as a sum of kinetic components (Lavorel, 1975):

$$L(t) = \sum_i L_i e^{-t/\tau_i},$$

where $L(t)$ is the *DF* intensity at time t after illumination has ceased, L_i is the amplitude of the i^{th} component, and τ_i is its lifetime.

The decay kinetics of *DF* in a time range from several microseconds to milliseconds after light excitation has been thought to reflect the recombination between the reduced primary quinone electron acceptor (Q_A^-) and the oxidized donor (P^+) of PS II that occurs after excitation of the reaction centres (Itoh and Murata, 1974; Lavorel, 1975). However, the electron equilibrium in reaction $ZP^+ \rightarrow Z^+P$ is reached within nanoseconds.

It is assumed that the emission in the microsecond to millisecond range is generated by recombination of $Z^+PQ_A^-$ (Van Gorkom and Donze, 1973; Jursinic, 1986).

DF components decaying in the millisecond time range are related to the kinetics of the electron transport in the acceptor (fast components) or the donor (slow components) side of PS II (Vesselovskii and Veselova, 1990). The slow components (in the seconds range and longer) of *DF* are associated with the recombination of S_2 and S_3 states of the oxygen-evolving system (Barbieri et al., 1970; Joliot et al., 1971; Lavorel, 1975) with Q_A^- and Q_B^-. Thus, the two long-lived components with times 1.5 and 25 s, registered in isolated chloroplasts (Rutherford and Inoue, 1984; Rutherford et al., 1984) are related to recombination of $S_2(S_3)$ states and reduced acceptors Q_A^- and Q_B^-, respectively.

5. Induction curves of delayed fluorescence

By using a phosphoroscope to register *DF*, one can obtain *DF* induction curves that, similar to the variable fluorescence transients, reflect the change from dark-adapted to light-adapted state of the sample. The shape of a *DF* induction curve depends on the sample type and its physiological state (Goltsev and Yordanov, 1997; Srivastava et al., 1999), as well as on the experimental protocol—duration of dark adaptation (Radenovic et al., 1985), temperature of registration (Markovic et al., 1999), actinic light intensity (V. Goltsev, unpublished data), and integrated decay range (Itoh and Murata, 1974; Malkin and Barber, 1978; Srivastava et al., 1999; Malkin et al., 1994). As a rule, *DF* is more sensitive (in at least some circumstances) to stress factors than fluorescence (Bjorn and Forsberg, 1979). Thus, *DF* is potentially a highly sensitive probe for the state of the photosynthetic organism (Jursinic, 1986).

DF transients have been shown to be driven by many mechanisms, including electrical and pH gradients (Wraight and Crofts, 1971), acceptor availability (Ruby, 1977), donor availability (Mar et al., 1975), and redox state of the oxygen-evolving system (Zankel, 1971; Van Gorkom and Donze, 1973; Barbieri et al., 1970; Goltsev et al., 1980). The delayed fluorescence induction curve, registered in a several minutes time period, encompasses two major phases—a fast one, taking place in the first second of induction, and a slow one, that can last for minutes. Each phase is shaped by several processes running at the same time (Goltsev and Yordanov, 1997). The fast phase of induction of the millisecond *DF* shows a very rapid increase to a level I (Itoh and Murata, 1973; Itoh et al., 1971b; Satoh and Katoh, 1983). Many authors attribute those initial phases of the induction to the changes of the electrical potential ($\Delta\psi$), depending on the state of the PS II reaction centre (Wraight and Crofts, 1971; Satoh and Katoh, 1983), since the light-induced potential difference and the proton gradient across the thylakoid membrane are thought to reduce the amount of activation energy necessary for the back reaction between Q_A^- and Z^+ to occur (Itoh et al., 1971a; Wraight and Crofts, 1971). On the other hand, the I level follows the extent of the variable component of fluorescence and has been suggested to be proportional to the amount of oxidized Q_A at the beginning of illumination (Itoh and Murata, 1973). Goltsev and Yordanov (1997) have distinguished two maxima in the fast phase of the *DF* induction curve (I_1 and I_2), appearing at times 33 and 150 ms and coinciding with the maximal rates of increase of $F_v(t)$ in the *O–I* and *D–P* phases, respectively. It has been assumed that *DF* originates from those PS II reaction centres that had completed a photochemical reaction during the preceding light pulse.

The *DF* increase to its maximum in the slow phase is usually attributed to the photoinduced transmembrane electrochemical gradient, ΔpH (Wraight and Crofts, 1971), but it probably reflects also the activation of the intersystem electron transfer in this induction period (Vesselovskii and Veselova, 1990; Malkin et al., 1994). The time course of *DF* after the maximum is possibly influenced by a number of dark photosynthetic processes (directly or indirectly modifying the characteristics of PS II). The decay is generally explained by a decrease in the membrane energization as a result of secondary cation efflux from thylakoids (Grigor'ev et al., 1982). The slow changes in the induction transient coincide with the SMT phase of the prompt fluorescence induction curve (Goltsev and Yordanov, 1997) which may be related to energy-dependent processes. These include: (a) changes in the thylakoid membrane structure (Govindjee and Papageorgiou, 1971; Papageorgiou, 1975), e.g. photoinduced state transition (Radenovic et al., 1994), affecting the quantum yield of fluorescence, or (b) energy-dependent fluorescence quenching as a result of activation of the violaxanthin deepoxidase and accumulation of zeaxanthin and antheraxanthin, which effectively quench the excited states of antenna chlorophylls (Horton and Ruban, 1994; Gilmore et al., 1998). Both mechanisms of quenching affect *PF* and *DF*.

Itoh (1980) has shown the inverse correlation between *PF* and *DF* (decaying in a few milliseconds) in the slow phases of induction under various conditions. Slow-delayed fluorescence (Itoh and Murata, 1974) has a completely different induction from fast-delayed fluorescence, i.e. a parallel correlation with the induction of prompt fluorescence (Clayton, 1969; Malkin and Barber, 1978). At present a clear correlation between *DF* decaying in several milliseconds and *PF* has not been established.

6. A model of the correlation of PF and DF

Since *PF* and *DF* are controlled by the same processes that occur during the transition from dark- to light-adapted state, the relation between both luminescence types could be predicted theoretically.

6.1. DF as a derivative function of PF

Measurement of the ms-*DF* induction kinetics requires the actinic light illuminating the sample to be chopped (either mechanically or electronically) to provide dark periods for registration. Within a given dark period (the first second of induction) the emission originates mainly from recombination of Z^+PQ^- states, accumulated during the preceding light period (Goltsev et al., 1998). Therefore, in order to yield *DF* emission during a dark period, the reaction centres must had been "open" (Q_A oxidized) in the preceding light period. Consequently, the *DF* intensity would be proportional to the fraction of "open" centres, $1–B$ (the fraction of "closed" centres B equals $[Q_A^-]/([Q_A]+[Q_A^-])$. The probability for recombination of Z^+PQ^- with excitation of the reaction centre chlorophyll can be defined as the term quantum efficiency of radiative recombination, r^*. It depends, among other factors, on thylakoid membrane energization (Wraight and Crofts, 1971), and on the redox state of Q_B. One can regard ZPQ_AQ_B, $ZPQ_AQ_B^-$ and $ZPQ_AQ_B^{=}$ as "light-emitting" states (able to generate $Z^+PQ_A^-$ states on illumination), whereas $ZPQ_A^-Q_B^{=}$ can be marked as "non-light-emitting". The earlier changes in the *DF* intensity during induction are related to transitions between these states (Goltsev and Yordanov, 1997).

Considering the above statements, for the *DF* intensity (L) we obtain

$$L \sim \varphi_{F_0} \times r^* \times (1-B) \times Abs \times \varphi_{P_0}, \tag{1}$$

where *Abs* is the excitation energy flux to each PS II RC, φ_{P_0} is the quantum yield of the primary photochemical reaction, and φ_{F_0} is the maximum quantum yield of fluorescence from PS II with open RC. We assume that the efficiency of electron transfer from pheophytin to Q_A is equal to 1. Otherwise, an additional constant could be introduced. The product of the last three parameters is the total photoinduced electron flux from the RC to the acceptor side of PS II.

Electrons transferred by the open RCs reduce the PS II acceptors and hence increase the variable chlorophyll fluorescence. For a short time interval of illumination (as in one light cycle of a phosphoroscope) the additional variable fluorescence, ΔF, produced by closing of open RCs would be then proportional to the electron flux through the PS II acceptor side:

$$\Delta F \sim K \times (\varphi_{F_m} - \varphi_{F_0}) \times (1-B) \times Abs \times \varphi_{P_0}, \tag{2}$$

where K is a variable depending on the momentary redox level of the acceptor pool beyond the Q_AQ_B site (mostly PQ in intact leaves) and its electron capacity, φ_{F_0} and φ_{F_m} are the quantum yields of fluorescence from PS II with open and closed RC, respectively.

The *DF* induction curve, which represents *DF* as a function of illumination time, $L(t)$, would be determined by the complex time courses of $r^*(t)$, $B(t)$ and $Abs(t)$. On the other hand, the *PF* induction curve is an integral function of ΔF. By comparing Eqs. (1) and (2) it may be assumed that during periods of insignificant changes of K the time course of $L(t)$ would follow the first derivative of $F(t)$, i.e. $L \sim F'(t)$. Indeed, our experimental results (see Fig. 2) show that in certain regions of the induction curves (I_1 and I_2) the *DF* maxima coincide with the maximal rates of *PF* increase, i.e. the first derivative of *PF* resembles *DF*. It may be suggested that in these time intervals the *DF* changes are mostly due to the redox level of the PS II acceptors (Q_A, Q_B).

6.2. Luminescence potential

The normalized (or relative) variable fluorescence, $V=(F_{(t)}-F_0)/(F_m-F_0)$, is proportional to the concentration of the closed centres when there is no connectivity between the RC. If connectivity is to be taken into account, the relative variable fluorescence, V, becomes a hyperbolic function of the fraction of closed reaction centres (B) (Havaux and Strasser, 1992).

Then the time function of the variable fluorescence, F_v, can be expressed as

$$\begin{aligned} F_v(t) &= F_{(t)} - F_0 = V \times (F_m - F_0) \\ &= V \times Abs \times (\varphi_{F_m} - \varphi_{F_0}). \end{aligned} \tag{3}$$

The quantum yields φ_{F_m} and φ_{F_0} are ratios of rate constants:

$$\varphi_{F_m} = \frac{k_f}{k_d + k_f} \quad \text{and} \quad \varphi_{F_0} = \frac{k_f}{k_d + k_f + k_p},$$

where k_d and k_f are the rate constants of dissipation of the excitation energy as heat and fluorescence, respectively, and k_p is the rate constant of photochemical trapping.

Then

$$\begin{aligned} \varphi_{F_m} - \varphi_{F_0} &= \frac{k_f}{k_d + k_f} - \frac{k_f}{k_d + k_f + k_p} \\ &= \frac{k_f(k_d + k_f + k_p) - k_f(k_d + k_f)}{(k_d + k_f)(k_d + k_f + k_p)} \\ &= \frac{k_f}{k_f + k_d} \times \frac{k_p}{k_d + k_f + k_p} = \varphi_{F_m} \times \varphi_{P_0}. \end{aligned}$$

Substituting in Eq. (3):

$$F_v = B \times Abs \times \varphi_{P_0} \times \varphi_{F_m}. \tag{4}$$

Dividing Eq. (1) by Eq. (4) we obtain the correlation

$$L/F_v \sim r^* \times (1-B)/B \times \varphi_{F_0} \times \varphi_{F_m}. \quad (5)$$

Eq. (5) shows that L/F_v is correlated with the ratio of oxidized to reduced states of the primary acceptor. On the other hand L/F_v is associated with the quantum efficiency of radiative recombination, r^*, which undergoes changes during the induction period as a result of the thylakoid membrane energization.

$$r^* = r_0^* \times \exp -\frac{E_a - F\Delta\psi + 2.3RT\Delta\mathrm{pH}}{kT}. \quad (6)$$

Here r_0^* is the fraction independent of the membrane potential, E_a is the activation energy of radiative recombination, $\Delta\psi$ is the membrane potential, k is the Boltzmann constant and the other symbols have their usual meanings.

Thus, the logarithm of L/F_v would be linearly proportional to the redox level of Q_A and the transmembrane potential

$$\ln(L/F_v) \sim \ln\frac{1-B}{B} - \frac{E_a - F\Delta\psi + RT\Delta\mathrm{pH}}{kT} + \ln\varphi_{F_0} - \ln\varphi_{F_m}. \quad (7)$$

Both the redox state of the PS II acceptors and the membrane energization control the efficiency of fluorescence radiation. The expression $\ln[(1-B)/B]$ is proportional to the redox potential of the couple Q_A/Q_A^- (according to the Nernst equation) and could be referred to as the driving force for electron transfer to Q_A (E'). Strasser (Strasser et al., 2000; Strasser and Tsimilli-Michael, 2001) derived in analogy to the Nernst equation a photosynthetic driving force which is the log of a so-called performance index, which can be calculated from the data of a fast fluorescence rise curve. This photosynthetic driving force can be decomposed into partial driving forces such as: due to the density of chlorophylls per leaf area, due to the density of RCs per chlorophyll, due to the photochemical reactions expressed with the maximum quantum yield of primary photochemistry and energy dissipation, and due to the driving force of the dark reactions, expressed as $\psi_0/(1-\psi_0) = (1-V)/V$, where ψ_0 is the probability for electron transport beyond Q_A^- per the rate of Q_A reduction. The driving force due to ψ_0 is here used as the first part of Eq. (7).

The second part of Eq. (7) is the additional energy needed for charge recombination in the $Z^+PQ_A^-$ complex. This energy barrier is reduced by the transmembrane electrochemical potential $\Delta\mu H^+ = F\Delta\psi - RT\Delta\mathrm{pH}$. Discarding all constants we come to

$$U_L = \ln(L/F_v) \sim E' + \Delta\mu H^+. \quad (8)$$

U_L can be named *luminescence potential* to indicate that it is actually a sum of potentials that determine the intensity of the two luminescence types—it modulates fluorescence quenching and is driving force for delayed fluorescence.

The correlation between luminescence and the luminescence potential can be plotted as $PF(U_L)$ and $DF(U_L)$. These would not be functions since the time courses $PF(t)$ and $DF(t)$ as well as $U_L(t)$ are not monotonous. They would rather be phase diagrams portraying the path that the sample follows during the transition from dark to light state. If linear regions exist in the diagram, it is most likely that only one of the two components (E' or $\Delta\mu H^+$) of U_L is changing the luminescence while the other is about constant. The slope of the line implies how sensitive the luminescence (PF or DF) is to the corresponding U_L component. On a $PF(U_L)$ plot linear regions should form where PF changes are due to the redox state or due to $\Delta\mu H^+$. These lines must be with negative slope because the oxidized Q_A and the membrane potential quench the fluorescence. On a $DF(U_L)$ plot linear regions with positive slope should appear where DF changes are due to E'. An exponential dependence is expected in the regions where $DF = f(\Delta\mu H^+)$.

The theoretically derived U_L can be calculated from experimental data if prompt and delayed fluorescence are detected simultaneously from the same sample during the induction period.

7. Experimental set-up

7.1. FL-2006—fluorometer for simultaneous registration of prompt and delayed chlorophyll fluorescence

The registration of the prompt and delayed fluorescence was carried out using an FL-2006 fluorometer, manufactured by TEST (Krasnoyarsk, Russia). It allows the simultaneous registration of induction kinetic curves of prompt and delayed chlorophyll fluorescence (Goltsev et al., 2001). A Becquerel-type disc phosphoroscope separates the PF and DF. The time period of one phosphoroscope work-cycle is 11.0 ms, including 5.15 ms "light period", when the PF is detected, another 5.15 ms "dark period" for registration of DF, and two non-detection intervals of 0.35 ms between them. The disc rotates at ca. 2000 rpm so that the time needed to fully open/close the aperture of the phosphoroscope does not exceed 0.2 ms. The fluorescence emitted during the "light period" is detected by a photomultiplier with a multialkaline photocathode of S20 type. During the "dark period", another photomultiplier detects the emitted delayed fluorescence. The anode signals are registered by a two-channel 10-bit ADC every 40 μs. All data points of one "dark period" (approx. 120) are averaged and stored as one DF induction point. 10 data points of one "light period" (the first one registered 300 μs after the aperture in front of the first

photomultiplier is fully open) are averaged and stored as one *PF* induction point. Thus, the time resolution of the registered induction curves of both *PF* and *DF* is about 11 ms.

A typical recording of the combined *PF*/*DF* signal obtained in the first 0.5 s after illumination onset is presented in Fig. 1.

The light source is covered by a shutter, which opens at the start of the measurements, during the first (dark) cycle of the disc, i.e. at the time of *DF* detection. The prompt fluorescence rise in the first registering cycle reflects the initial phase of the induction transient, that corresponds to the *O–J* rise observed with high resolution fluorometers (Strasser et al., 1995) (for comparison see open-symbol curves in Fig. 1, inset). Since the time needed to open the illuminating window is 0.2 ms and registration starts afterwards, the exact value of F_0 cannot be measured. Instead, the average of the first 10 points is stored as F_0.

The delayed fluorescence emitted during a dark period decays exponentially and the data stored as one induction point for each period is an average of all collected points (see Fig. 1, inset).

7.2. Plant material

To illustrate the luminescence behaviour of samples with different structure of the photosynthetic apparatus we have used two types of barley plants—wild-type and a chlorophyll *b*-less mutant *chlorina f2*. The mutation in *chlorina f2* involves a nuclear gene encoding the synthesis of chlorophyll *b*. As a result, the mutant is deficient in most of the LHCII polypeptides and some PS I polypeptides (Bellemare et al., 1982). According to the present nomenclature of photosynthetic polypeptides, *chlorina f2* and several similar barley mutants completely lack Lhca4, Lhcb1 and Lhcb6 while Lhcb2, Lhcb3, and Lhcb4 are in reduced quantities. The proteins Lhca1, 2 and 3, Lhcb5, and PsbS are normally present as in the wild type (Bossmann et al., 1997). The mutation results in increased ratio of stromal to granal thylakoids (Goodchild et al., 1966; Bassi et al., 1985) and reduced surface charge density of the thylakoid membrane (Chow et al., 1991). The reduced antenna size results in faster fluorescence decay and decreased F_m/F_0 ratio (Gilmore et al., 1996).

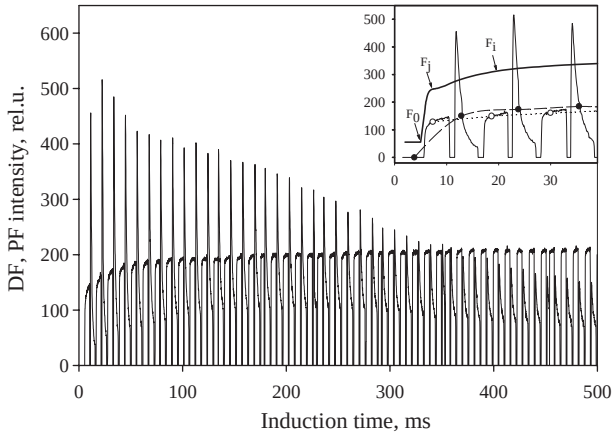

Fig. 1. Combined recording of prompt and delayed fluorescence registered through two ADC channels. The signal is a sequence of alternating *PF* and *DF* measurements (120 points each), separated by dead intervals. Inset—the same diagram, presented in expanded time scale. The averaged values form both integral induction curves are shown as dotted lines (*PF*—open circles, *DF*—filled circles). The thick solid line shows the *PF* induction trace, registered using Handy PEA (Hansatech Instruments, UK), at approximately the same excitation light intensity (1200 μmol m^{-2} s^{-1}).

Wild-type and *chlorina f2* plants were grown as a hydroponics culture in Knop's solution for 8 days in a climatic chamber at controlled temperature (25°C/20°C, day/night) and light (50 μmol photons m^{-2} s^{-1}, 12 h day^{-1}). Before measurements, whole plants were dark-adapted for 1 h. Leaf segments were transferred in the measuring chamber and kept for 1 min in the dark at the experimental temperature of 20°C.

8. Analysis of experimental data

8.1. Induction curves of PF and DF

Upon illumination of photosynthetic samples initially adapted in the dark, both prompt and delayed fluorescence undergo typical changes, referred to as induction transients (Malkin, 1977; Krause and Weis, 1991; Radenovic et al., 1994; Govindjee, 1995). The *PF* and *DF* induction curves for leaves from barley plants are shown in Fig. 2.

The nature of luminescence induction involves fast changes in the millisecond time interval and much slower ones, observed in seconds and minutes. In order to picture all phases in the transient, a logarithmic time scale is used. The fluorescence induction curve in a 3 min time period, assembled from single points every 11 ms, depicts most known induction phases—F_0, F_i, F_p, F_s, F_m, F_t (OIPSMT phases, see Papageorgiou, 1975 for a review). As it was noted before, there is a certain variable fluorescence part in the measured F_0 raising it higher than the actual value. The *J* peak would appear at or before the time of the first registered point of the induction curve (see Fig. 1, inset).

The induction curve of *DF* as a whole can be regarded as the combined result of at least six superimposed peaks, denoted in order of their occurrence on the timescale as I_1–I_6. The I_2, I_4 and I_6 peaks correspond to the *B*, *C* and *D* peaks in the nomenclature of Radenovic et al. (1994).

The simultaneous recording of both types of luminescence allows the transient phases to be related by their times. The first two maxima observed in the *DF*

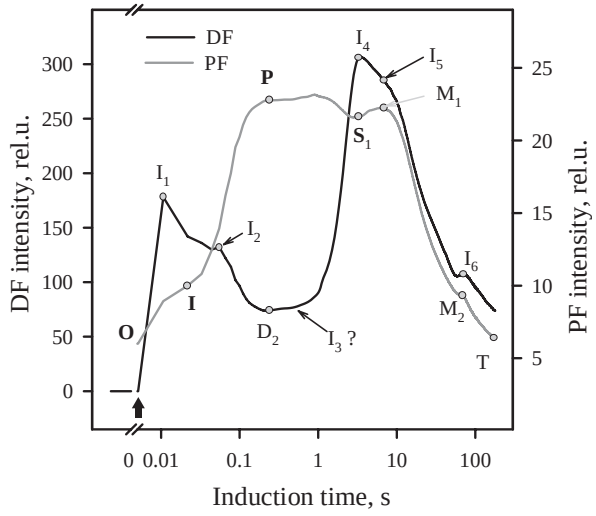

Fig. 2. Time course of simultaneously recorded integrated prompt (grey) and delayed (black) chlorophyll fluorescence of leaf discs from 1 h dark-adapted plants of barley. Actinic light intensity was 1200 μmol m^{-2} s^{-1}. Grey and black arrows show the characteristic points of the both induction curves. The wide arrow (⇑) indicates the time when the actinic light was switched on.

intensity in the sub-second range of the induction period (denoted as I_1 and I_2) coincided with the moments of maximal rate of F_0–F_i and of F_i–F_p increase in *PF*. We have proposed previously that their amplitudes reflect the redox transitions on the acceptor side of PS II (Goltsev and Yordanov, 1997). Such behaviour confirms the validity of Eqs. (1) and (2) and the assumption that in certain regions of the induction $DF(t)$ resembles the first derivative function of $PF(t)$.

A shoulder noted as I_3 is sometimes found at the end of the fast phase. Its origin and the conditions in which it appears are still uncertain. We have found that I_3 is mainly due to the slow millisecond components of *DF* (Zaharieva and Goltsev, 2003). A well-pronounced dip, D_2, is usually observed after I_2. The minimum is reached at the same time as F_p. Therefore, it may be a result of closure of the PS II RCs during the PQ pool reduction (Goltsev and Yordanov, 1997). The profound increase in the slow phase (D_2–I_4) of the *DF* induction curve takes place at the same time with the *PF* transition *P*–*S*. The later *DF* maximum, I_5, is related to the *PF* transition *S*–M_1 in a way similar to the fast phase *DF* maxima. The appearance of the late maxima in DF (I_4 and I_5) in the seconds time range of the induction curve can be related to the photoinduced proton gradient as well as to the initiation of the photosynthetic dark reactions (Wraight and Crofts, 1971; Gaevskii and Morgun, 1993). Energization of the thylakoid membranes quenches the fluorescence in the *P*–*S* phase of *PF* transients where the *DF* increase (D_2–I_4) is parallel to a *PF* decrease. I_6 appears in the slow phase usually at temperatures above 30°C. It can be assumed that I_6 is a result of activation of the Calvin–Benson cycle, which is initiated by ATP and NADPH accumulation (Zaharieva et al., 2001).

PF and *DF* induction curves are, to some degree, similar in both the wild type and *chlorina f2* mutant (data not shown). The *PF* intensity is considerably lower in the mutant due to the reduced chlorophyll content. However, *DF* intensity is unaffected. This may be explained by the compensatory increase in the number of PS II centres (Ghirardi et al., 1986; Ghirardi and Melis, 1988) and the increased ratio of PS II reaction centres per chlorophyll molecules as the result of reduced PS II antenna size (Zaharieva et al., 1999). Differences with the wild type are also found in the shape of the induction curves, reflecting structural changes in the antenna complexes (see below). The lower rate of electron transport through PS II in *chlorina f2* (Havaux and Tardy, 1997) results in changes in the fast phase of *DF* induction, which may reflect the redox state of the PS II acceptors (Goltsev and Yordanov, 1997).

8.2. Time course of the L/F_v ratio during the induction

Fig. 3 shows the time curves of $L/F_v = f(t)$ for barley leaves of wild type and *chlorina f2*. According to Eq. (5), the changes in this ratio during the induction period are determined by the redox state of the PS II acceptors and by factors influencing the yield of radiative recombination of charges in the RC. The time course of the curves resembles *DF* induction curves but some phases are

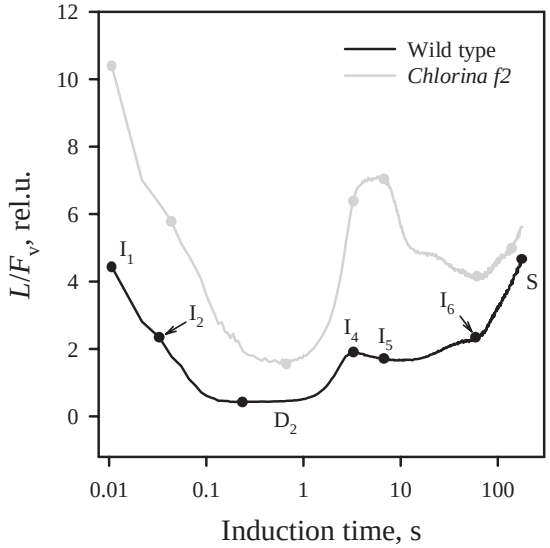

Fig. 3. Time course of the luminescent ratio L/F_v measured in leaves of barley wild-type and *chlorina f2* mutant. The measuring conditions are as in the legend to Fig. 2. *L* is *DF* intensity normalized to the maximal value. F_v is normalized variable fluorescence, $F_v = (F_{(t)} - F_0)/(F_m - F_0)$. The points denoted as I_1, I_2, D_2, I_4, I_5, I_6 and *S* show characteristic points of *DF* induction (Fig. 2) and the moments of induction when phase trajectories (see Fig. 4B and D) change their direction.

more emphasized. The I_4 and I_6 maxima in the slow phase are more profound in wild-type plants. The slow rise of L/F_v at the end of the registration period is perhaps related to the reoxidation of the PQ pool due to activation of the dark reactions.

The mutant has reduced antenna size compared to the wild type. Therefore the excitation energy input flux to the reaction centres is smaller in the mutant. The acceptor-side electron carriers should remain less reduced, hence the increased $(1-B)/B$ and higher values of L/F_v for the mutant in the entire induction period. The latter might be related to higher density of PS II reaction centres in *chlorina f2* due to reduced PS II antenna size. If the D_2 minimum is due to PQ pool reduction, then the slower closure of the RCs (and lower rate of the PQ pool reduction) results in decelerated I_2–D_2 decay in the mutant. The D_2 dip in the wild type is wider because the RCs remain closed for a longer time.

Activation of PS I, which is inactive in the dark (Satoh et al., 1977), is accompanied by a *DF* increase in the slow phase—D_2–I_4. It may be due to the thylakoid membrane energization or reoxidation of the previously reduced PQ pool, i.e. opening of PS II RCs. The relative amplitude of this phase (ratio $(I_4–D_2)/D_2$, a measure of the enhancement of *DF*) is the same for wild type and *chlorina f2*—4.6. It is therefore concluded that the increase of L/F_v in the slow phase is most probably a result of energization of the membrane rather than reopening of the RCs. Moreover, the observed similarity indicates that energization does not depend on the antenna size. On the other hand, the rise of L/F_v in the wild type ends in 2 s while in the mutant it continues for 5 s and I_4 is considerably delayed. It is possible that after the initial generation of transmembrane gradient, the light emission is further enhanced in the mutant by partial reopening of the reaction centres due to activation of the linear electron transport through PS I, as the rate of electron transport through PS II is low (Highkin and Frenkel, 1962; Boardman and Highkin, 1966) and the number of PS I RCs is greater than in the wild type (Härtel and Lokstein, 1995).

8.3. Phase diagrams—*V* vs. U_L and *L* vs. U_L

The luminescence potential $U_L = \ln(L/F_v)$ derived in the theoretical section was calculated from the experimental data. Fig. 4 shows the variable and delayed fluorescence of wild-type barley and *chlorina f2* plotted against U_L. Such phase diagrams show how prompt and delayed fluorescence depend on the two components of U_L. As it was proposed, linear regions indicate periods where only one of the two factors of U_L (E' or $\Delta\mu H^+$) is responsible for the luminescence changes, for instance $V = b_0 + b_1E'$. The linear

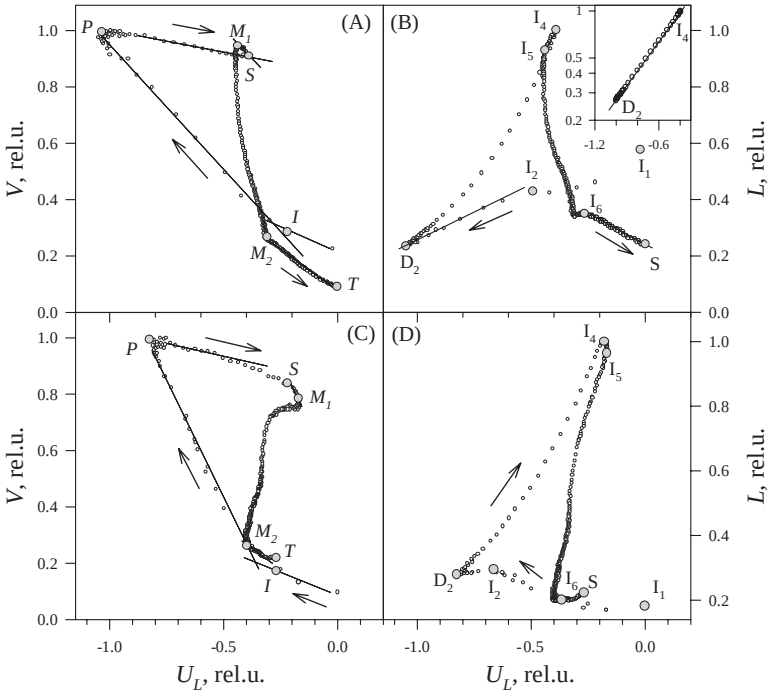

Fig. 4. The course of the changes of relative variable, *V* (A, C) and delayed, *L* (B, D) chlorophyll fluorescence during dark–light transition as a dependence on luminescence potential ($U_L = E' + \Delta\mu H^+$) in leaves of barley—wild-type (A, B) and *chlorina f2* mutant (C, D). Grey circles represent characteristic points of *PF* and *DF* induction curves as in Fig. 2. Data are from Fig. 3. All data are normalized to the corresponding maximal values. Experimental conditions were as in Fig. 1. Inset: part of experimental points from D_2 to I_4 is presented in semi-logarithmic scale. The straight line shows linear regression of the experimental points.

regression coefficients b_0 and b_1 calculated from $V(U_L)$ are presented in Table 1.

The *I–P* section can be related to two different processes. It can be photochemical, i.e. the fluorescence rise is due to photoinduced reduction of the PS II electron acceptors. Or, it may reflect changes in the electrical potential (probably generated by PS I) as shown for saturating light conditions by Vredenberg and Bulychev (2002). At our experimental conditions, where the actinic light intensity is relatively low, U_L monotonously decreased from the start of induction up to *P*, pointing that the fluorescence rise in the *I–P* phase is most probably of photochemical nature.

The slope b_1 represents a proportion between the amount of reduced acceptors and the *PF* increase and should depend on the number of antenna chlorophylls per one electron transport chain. The results show that b_1 for *chlorina f2* mutants is about two-fold higher than for the wild type. The meaning is that during the induction period the redox potential changes in the mutant are two-fold smaller. Simpson et al. (1985) have shown that the time needed to reach the half-maximal variable fluorescence in intact leaves in the presence of diuron, used as a measure of the PS II antenna size, is two- to four-fold greater in *chlorina f2* mutants.

The first few points at the start of the phase curve deviate from the *I–P* line and this section is denoted as *O–I* (please note that *O* means only the first registered fluorescence level). The course of the *PF* and *DF* changes in this region could be dictated by the dissipation of the photoinduced electrical gradient, formed immediately after the actinic light onset. The slope of the *O–I* line is much smaller than *O–P*, especially for *chlorina f2*, and is closer to the slope of *P–S*, which is related to the membrane energization (see below).

Chlorina f2 lacks LHCII-bound pigments but has greater amount of LHCI pigments (Härtel and Lokstein, 1995). The longer *O–I* section in the mutants is possibly due to the greater number of active PS I units—PS I generates $\Delta\Psi$ in the first milliseconds of the induction period (Satoh and Katoh, 1983).

The third phase, *P–S*, is characterized by a *PF* decrease (Fig. 4A and C) and a *DF* increase (region D_2–I_4, Fig. 4B and D). This transition matches in time with the photoinduced generation of transmembrane proton gradient (Briantais et al., 1979) while the redox state of the electron carriers remains more or less constant. The slope of the estimated line in the *P–S* region is approximately the same as of the *O–I* line but in the inverse direction—toward formation, rather than dissipation of the potential. The rise of U_L is determined predominantly by the exponential dependence of r^* on $\Delta\mu H^+$ and the drop of *PF*—by the energy-dependent quenching (Briantais et al., 1979; 1980).

It must be stressed that the estimated slopes are close for both investigated samples (less than 13% difference), which shows the relative independence on the structure of the antenna. At the end of the *P–S* phase the *chlorina f2* curve is not linear but bends down. This might be a result of an additional quenching process, e.g. photochemical quenching due to a faster activation of PS I and reoxidation of PQ.

The slope of the curve in the S–M_1 section is equal to that of *I–P* for both plant types, but in the mutant the trajectory moves in the opposite direction. The following speculations may explain this occurrence. After proton gradient has formed in the wild type, the ATP-synthase is activated and the PS II acceptors are once again reduced. This might be due to the depletion of the oxidized acceptor $NADP^+$ before the Calvin–Benson cycle reactions have started. As a result, fluorescence rises and *DF* drops. However in the mutant after formation of the proton gradient the RCs are opened in accordance with the previously proposed analysis of Fig. 3 that pointed to a reopening of PS II centres during the formation of $\Delta\mu H^+$ due to the decelerated electron flow.

The M_1–M_2 section of the $V(U_L)$ plot is nonlinear and we cannot assume that a single process controls the *V* changes. On the other hand, a large drop in *V* is observed while U_L is virtually constant. Therefore it is likely that the quenching of fluorescence in this section is due to processes not involved in U_L. They cannot be

Table 1
Linear regression coefficients ($U_L = b_0 - b_1 V$) of different linear regions of the phase diagrams *V* vs. U_L for leaves of wild-type and *chlorina f2* mutant of barley

Region of phase	Wild type			*Chlorina f2*		
diagram	b_0	b_1	r^2	b_0	b_1	r^2
O–I	0.21	−0.36	0.98	0.09	−0.33	0.93
I–P	0.07	−0.88	0.99	−0.40	−1.66	0.99
P–S	0.86	−0.16	0.98	0.84[a]	−0.18[a]	0.91
S–M_1	0.58	−0.84	0.94	0.49	−1.68	0.88
M_2–*T*	0.08	−0.59	0.99	0.03	−0.59	0.95

Data are from Fig. 4. *V* is relative variable fluorescence.
[a] Regression was made only for the linear part of the *P–S* region.

identified with certainty so far although in this part of the phase curve the differences between the wild type and mutants are bigger. The *PF* drop in this late phase of induction is possibly due to a non-photochemical quenching associated with the violaxanthin turnover, which is more pronounced in the mutants (Andrews et al., 1995).

The final phase M_2–T is linear again. During this period most of the transient processes come to a steady (light-adapted) state. The slope is virtually the same for wild type and *chlorina* and arranges between the I–P and P–S slopes. It might be speculated that during the later phases of induction the changes in the fluorescence yield are not due to the redox state changes of the electron acceptors but to other quenching mechanisms of non-photochemical nature.

The correlation between the photoinduced changes of the luminescence potential and the delayed fluorescence is shown in Fig. 4, plots B and D. The course of the phase trajectory in the initial regions (I_1–I_5) is in the reverse direction compared to the *PF* trajectory (O–M_1). On the contrary, in the final part *PF* and *DF* show almost identical dependence on U_L. It seems that in the early moments of induction *PF* and *DF* are controlled solely on the luminescence potential—i.e. openness of reaction centres and membrane potential. Different processes take place in the later phases of induction that modify *PF* and *DF* in a similar way, most probably via φ_{F_0} and φ_{F_m}. These could include zeaxanthin formation, excitation energy spillover towards PS I or migration of LHCII into the stromal thylakoids.

The luminescence potential drops rapidly from maximum to minimum during the first second of induction (O–P, I_1–D_2). The delayed fluorescence changes linearly with U_L in the I_2–D_2 section. In the I_1–I_2 section *DF* exhibits a decrease in the wild type and an increase in *chlorina*. The drop might be explained with the dissipation of the transmembrane electrical gradient, while the increase could be because light-emitting states ($ZPQ_AQ_B^-$) are accumulating with time. The smaller PS II antennae in the mutants make this process much slower than in the wild type.

An exponential rise of *DF* with U_L is observed in the D_2–I_4 region. This curve deconvolutes in a semi-logarithmic scale (see inset of Fig. 4B) into a straight line with slope 0.93 for wild type and 0.91 for mutant plants.

The phase portrait as a whole, like the induction curves of both types of luminescence, illustrates the transition of the photosynthetic system between two phase states—dark- and light-adapted state. As it can be seen from Figs. 3 and 4, the transition route in different samples has some common characteristic regions and some specifics (differences in the region I–P, M_1–T and I_1–D_2, I_4–S). They must reflect the specificity of the state-change due to structural differences between the samples.

It is believed (Tsimilli-Michael et al., 1996) that when a change in the environmental conditions (e.g. light intensity) occurs, the system undergoes structural changes in order to improve its fitness to the new environment and achieve maximal performance. That is why in optimally functioning systems (native plants) the photosynthetic efficiency and hence the dissipated energy (estimated by the steady-state fluorescence) remains constant in a wide range of light intensities.

In accordance with this concept, the steady-state level of fluorescence in the light state F_t of wild-type plants is close to or even lower than F_0 (Havaux et al., 1991), while in mutant plants $F_t > F_0$. If we regard additional parameters (such as L/F_v) as characterizing the photosynthetic state the same conclusion can be made: after induction is completed the parameter returns to its initial values only in the wild type whereas in the *chlorina* mutant the initial level cannot be reached. We therefore can assume that *chlorina f2* plants cannot adapt in the light to reach the initial state they had in the dark as the wild type does. Each adaptation is an optimization process limited by the capacity of the system to respond to environmental changes (Strasser, 1988). Therefore, we conclude that the mutant is less adaptable to continuous light than the wild type.

The analysis of the relation between the *PF* and *DF* changes during the induction period was meant to provide an idea of the possibilities to explore the information contained in the induction curves for a better examination of any photosynthetic system. It is obvious that in spite of the large amount of information, its interpretation is extremely difficult because the complexity of the system and the interactions of many concurrent processes. In order to better understand the acquired parameters, a theory must be built that considers not only the integral *DF* induction signal but also the role of independent decay components during the induction period.

9. Conclusions

A theoretical model was developed, which predicts the correlations between prompt and delayed fluorescence registered simultaneously. A new parameter was derived from the ratio between the delayed fluorescence and the variable fluorescence, named luminescence potential, U_L. It is proportional to the sum of the redox potential of the primary acceptor of PS II and the transmembrane electrochemical potential and represents the driving force for the millisecond delayed light emission. The analysis of the relation between U_L and the two luminescence types allowed us to verify the sequence of events controlling *DF* which occur in the thylakoid membranes during the transition from dark to light. It is

possible to resolve which processes dominate in the formation of *PF* and *DF* in different phases of the induction and to explain why *PF* and *DF* are inversely correlated in some section and parallel in other.

Acknowledgements

We are grateful to David Simpson for kindly providing us with the *chlorina f2* mutant seeds and to Prof. Govindjee for critically reading the manuscript. We thank the Swiss National Science Foundation for financial support (SCOPES 2000–2003 grant No. 7BUPJ062408.00/1).

References

Amesz, J., Van Gorkom, H.J., 1978. Delayed fluorescence in photosynthesis. Annu. Rev. Plant Physiol. 29, 470.

Andrews, J.R., Fryer, M.J., Baker, N.R., 1995. Consequences of LHC II deficiency for photosynthetic regulation in *chlorina* mutants of barley. Photosynth. Res. 44, 81–91.

Barbieri, G., Delosme, R., Joliot, P., 1970. Comparaison entre l'emission d'oxygene et l'emission de luminescence a la suite d'une serie d'eclairs saturants. Photochem. Photobiol. 12, 197–206.

Bassi, R., Hinz, U., Barbato, R., 1985. The role of the light harvesting complex and photosystem II in thylakoid stacking in the *chlorina-f2* barley mutant. Carlsberg Res. Commun. 50, 347–367.

Bellemare, G., Bartlett, S.G., Nam-Hai, C., 1982. Biosynthesis of chlorophyll a/b-binding polypeptides in wild type and the chlorina f2 mutant of barley. J. Biol. Chem. 257, 7762–7767.

Bjorn, C.D., Forsberg, A.S., 1979. Imaging by delayed light emission (phytoluminography) as a method for detecting damage of the photosynthetic system. Physiol. Plant. 47, 215–222.

Boardman, N.K., Highkin, H.R., 1966. Studies on barley mutant lacking chlorophyll b. I. Photochemical activity of isolated chloroplasts. Biochim. Biophys. Acta 126, 189–199.

Bossmann, B., Knoetzel, J., Jansson, S., 1997. Screening of *chlorina* mutants of barley (*Hordeum vulgare L.*) with antibodies against light-harvesting proteins of PS I and PS II: absence of specific antenna proteins. Photosynth. Res. 52, 127–136.

Briantais, J.-M., Vernotte, C., Picaud, M., Krause, G.H., 1979. A quantitative study of the slow decline of chlorophyll *a* fluorescence in isolated chloroplasts. Biochim. Biophys. Acta 548, 128–138.

Briantais, J.-M., Vernotte, C., Picaud, M., Krause, G.H., 1980. Chlorophyll fluorescence as a probe for the determination of the photo-induced proton gradient in isolated chloroplasts. Biochim. Biophys. Acta 591, 198–202.

Butler, W.L., 1977. Chlorophyll fluorescence: a probe for electron transfer and energy transfer. In: Ttrebst, A., Avron, M. (Eds.), Photosynthesis I. Photosynthetic Electron Transport and Photophosphorylation. Berlin, Springer-Verlag, pp. 149–167.

Chow, W.S., Miller, C., Anderson, J.M., 1991. Surface charges, the heterogenous lateral distribution of the two photosystems, and thylakoid stacking. Biochim. Biophys. Acta 1057, 69–77.

Clayton, R.K., 1969. Characteristics of prompt and delayed fluorescence from spinach chloroplasts. Biophys. J. 9, 60–76.

deVault, D., Govindjee, Arnold, W., 1983. Energetics of photosynthetic glow peaks. Proc. Natl. Acad. Sci. USA 80, 983–987.

Gaevskii, N.A., Morgun, V.N., 1993. Use of variable fluorescence and delayed light emission to studies of plant physiology. Plant Physiol. (Moscow) 40, 136–145.

Ghirardi, M.L., Melis, A., 1988. Chlorophyll *b* deficiency in soybean mutants: effect on photosystem stoichiometry and chlorophyll antenna size. Biochim. Biophys. Acta 932, 130–137.

Ghirardi, M.L., McCanley, S.W., Melis, A., 1986. Photochemical apparatus organization in the thylakoid membrane of *Hordeum vulgare* wild type and chlorophyll b-less *chlorina f2* mutant. Biochim. Biophys. Acta 851, 331–339.

Gilmore, A.M., Hazlett, T.L., Debrunner, P.G., Govindjee, 1996. Photosystem II chlorophyll *a* fluorescence lifetimes and intensity are independent of the antenna size differences between barley wild-type and *chlorina* mutants: photochemical quenching and xanthophyll cycle-dependent nonphotochemical quenching of fluorescence. Photosynth. Res. 48, 171–187.

Gilmore, A., Shinkarev, V.P., Hazlett, T.L., Govindjee, 1998. Quantitative analysis of the effects of intrathylakoid pH and the Xanthophyll cycle pigments on chlorophyll *a* fluorescence lifetime distributions and intensity in thylakoids. Biochemistry 37, 13582–13593.

Goltsev, V.N., Yordanov, I.T., 1997. Mathematical model of prompt and delayed chlorophyll fluorescence induction kinetics. Photosynthetica 33, 571–586.

Goltsev, V., Ortoidze, T., Sokolov, Z., Matorin, D., Venediktov, P., 1980. Delayed luminescence yield kinetics in flash illuminated green plants. Plant Sci. Lett. 19, 339–346.

Goltsev, V., Traikov, L., Hristov, V., 1998. Effects of exogenous electron acceptors on kinetic characteristics of prompt and delayed fluorescence in atrazine inhibited thylakoid membranes. In: Garab, G. (Ed.), Photosynthesis: Mechanisms and Effects. Kluwer Academic Publishers, Dordrecht, pp. 3885–3888.

Goltsev, V., Yordanov, I.T., Stefanov, D., Zaharieva, I., Lambrev, P.H., Strasser, R.J., 2001. Simultaneous analysis of variable and delayed chlorophyll fluorescence during induction period in photosynthetic apparatus. In: Proceedings of the 12th International Congress on Photosynthesis. CSIRO Publishing, Colingwood.

Goodchild, D.J., Highkin, H.R., Boardman, N.K., 1966. The fine structure of chloroplasts in a barley mutant lacking chlorophyll *b*. Exp. Cell Res. 43, 684–688.

Govindjee, 1995. Sixty-three years since Kautsky: chlorophyll *a* fluorescence. Aust. J. Plant Physiol. 22, 131–160.

Govindjee, Papageorgiou, G., 1971. Chlorophyll fluorescence and photosynthesis: fluorescence transients. In: Giese, A.C. (Ed.), Photophysiology. Academic Press, New York, pp. 1–46.

Grigor'ev, Yu.S., Morgun, V.N., Gol'd, V.M., Gaevskii, N.A., 1982. Study of light-induced changes of millisecond delayed light emission in pea chloroplasts. Biofizika 27, 973–976.

Härtel, H., Lokstein, H., 1995. Nonphotochemical quenching of chlorophyll fluorescence in leaves: influence of photosystem II antenna size and violaxanthin de-epoxidation. In: Mathis, P. (Ed.), Photosynthesis: from Light to Biosphere. Kluwer Academic Publishers, Dordrecht, pp. 291–294.

Havaux, M., Strasser, R.J., 1992. Dynamics of electron transfer within and between PS II reaction center complexes indicated by the light-saturation curve of in vivo variable chlorophyll fluorescence emission. Photosynth. Res. 31, 149–156.

Havaux, M., Tardy, F., 1997. Thermostability and photostability of photosystem II in leaves of the *chlorina-f2* barley mutant deficient in light-harvesting chlorophyll a/b protein complexes. Plant Physiol. 113, 913–923.

Havaux, M., Strasser, R.J., Greppin, H., 1991. Effects of incident light intensity on the yield of steadystate chlorophyll fluorescence in intact leaves. An example of bioenergetic homeostasis. Environ. Exp. Bot. 31, 23–32.

Highkin, H.R., Frenkel, A.W., 1962. Studies of growth and metabolism of a barley mutant lacking chlorophyll *b*. Plant Physiol. 37, 814–820.

Horton, P., Ruban, A.V., 1994. The role of light-harvesting complex II in energy quenching. In: Baker, N.R., Bowyer, J.R. (Eds.), Photoinhibition of Photosynthesis: From Molecular Mechanisms to the Field. BIOS Scientific Publishers, Oxford, pp. 111–128.

Itoh, S., 1980. Correlation between the time course of millisecond delayed fluorescence and that of prompt fluorescence at low temperature in uncoupled spinach chloroplasts. Plant Cell Physiol. 21, 873–884.

Itoh, S., Murata, N., 1973. Correlation between delayed light emission and fluorescence of chlorophyll *a* in system II particles derived from spinach chloroplasts. Photochem. Photobiol. 18, 209–218.

Itoh, S., Murata, N., 1974. Studies on the induction and decay kinetics of delayed light emission in spinach chloroplasts. In: Avron, M. (Ed.), Proceedings of the Third International Congress on Photosynthesis. Elsevier, Amsterdam, pp. 115–126.

Itoh, S., Katoh, S., Takamiya, A., 1971a. Studies on the delayed light emission in spinach chloroplasts. II. Participation of primary electron donor and acceptor of photoreaction II in producing the delayed light emission. Biochim. Biophys. Acta 245, 121–128.

Itoh, S., Murata, N., Takamiya, A., 1971b. Studies on the delayed light emission in spinach chloroplasts. I. Nature of two phases in development of the millisecond delayed light emission during intermittent illumination. Biochim. Biophys. Acta 245, 109–120.

Joliot, P., Joliot, A., Bouges, B., Barbieri, G., 1971. Studies of system II photocenters by comparative measurements of luminescence, fluorescence, and oxygen emission. Photochem. Photobiol. 14, 287–305.

Jursinic, P.A., 1986. Delayed fluorescence: current concepts and status. In: Govindjee, Amesz, J., Fork, D.C. (Eds.), Light Emission by Plants and Bacteria. Academic Press, Orlando, pp. 291–328.

Kautsky, H., Hirsch, A., 1931. Neue Versuche zur Kohlensaureassimilation. Naturwissenschaften 19, 964.

Krause, G.H., Weis, E., 1991. Chlorophyll fluorescence and photosynthesis: the basics. Annu. Rev. Plant. Physiol. Plant Mol. Biol. 42, 313–349.

Lavorel, J., 1975. Luminescence. In: Govindjee (Ed.), Bioenergetics of Photosynthesis. Academic Press, New York, pp. 223–317.

Malkin, S., 1977. Delayed luminescence. In: Trebst, A., Avron, M. (Eds.), Photosynthesis I: Photosynthetic Electron Transport and Photophosphorilation. Springer, Berlin, pp. 473–491.

Malkin, S., Barber, J., 1978. Induction patterns of delayed luminescence from isolated chloroplasts. I. Response of delayed luminescence to prompt fluorescence yield. Biochim. Biophys. Acta 502, 524–541.

Malkin, S., Bilger, W., Schreiber, U., 1994. The relationship between millisecond luminescence and fluorescence in tobacco leaves during the induction period. Photosynth. Res. 39, 57–66.

Mar, T., Brebner, J., Roy, G., 1975. Induction kinetics of delayed light emission in spinach chloroplasts. Biochim. Biophys. Acta 376, 345–353.

Markovic, D.Z., Radenovic, C.N., Rafailovic, L., Zerajic, S.A., Jeremic, M., Markovic, M.B., 1999. Temperature dependence of delayed fluorescence induction curve transients. Gen. Physiol. Biophys. 18, 257–267.

Papageorgiou, G., 1975. Chlorophyll fluorescence: an intrinsic probe of photosynthesis. In: Govindjee (Ed.), Bioenergetics of Photosynthesis. Academic Press, New York, pp. 319–371.

Radenovic, C.N., Jeremic, M., Fidler, D., Markovic, D.Z., Vucinic, Z., 1985. A kinetic study of delayed fluorescence induction its dependence on preceding darkness. Period. Biol 87, 304–306.

Radenovic, C.N., Markovic, D.Z., Jeremic, M., 1994. Delayed chlorophyll fluorescence in plant models. Photosynthetica 30, 1–24.

Ruby, R.H., 1977. Delayed fluorescence from *Chlorella*. II. Effects of electron transport inhibitors DCMU and NH_2-OH. Photochem. Photobiol. 26, 293–298.

Rutherford, A.W., Inoue, Y., 1984. Oscillation of delayed luminescence from PSII: recombination of $S_2Q_B^-$ and $S_3Q_B^-$. FEBS Lett. 165, 163–170.

Rutherford, A.W., Govindjee, Inoue, Y., 1984. Charge accumulation in leaves studied by thermoluminescence and delayed light emission. Proc. Natl. Acad. Sci. USA 81, 748–752.

Satoh, K., Katoh, S., 1983. Induction kinetics of millisecond-delayed luminescence in intact *Bryopsis* chloroplasts. Plant Cell Physiol. 24, 953–962.

Satoh, K., Yamagishi, A., Katoh, S., 1977. Fluorescence induction in chloroplasts isolated from green alga, *Bryopsis maxima*. II. Induction of cytochrome *f* photooxidation and the DPS transient in fluorescence induction. In: Miyachi, S., Katoh, S., Fujita, Y., Shibata, K. (Eds.), Photosynthetic Organelles. Special Issue of Plant Cell Physiol No. 3. Japanese Society of Plant Physiologists and Center for Academic Publications Japan, Tokyo, pp. 75–86.

Shinkarev, V.P., Govindjee, 1993. Insight into the relationship of chlorophyll *a* fluorescence to the concentration of its natural quenchers in oxygenic photosynthesis. Proc. Natl. Acad. Sci. USA 90, 7466–7469.

Simpson, D.J., Machold, O., Hoyer-Hensen, G., von Wettstein, D., 1985. Chlorina mutants of barley (*Hordeum vulgare* L.). Carlsberg Res. Commun. 50, 223–238.

Srivastava, A., Strasser, R.J., Govindjee, 1999. Greening of peas: parallel measurements of 77 K emission spectra, OJIP chlorophyll *a* fluorescence transient, period four oscillation of the initial fluorescence level, delayed light emission, and P700. Photosynthetica 37, 365–392.

Stirbet, A.D., Strasser, R.J., 2001. The possible role of pheophytine in the fast fluorescence rise OKJIP. In: Proceedings of the 12th International Congress on Photosynthesis. CSIRO Publishing, Colingwood.

Strasser, R.J., 1988. A concept for stress and its application in remote sensing. In: Lichtenthaler, H.K. (Ed.), Applications of Chlorophyll Fluorescence. Academic Press, The Netherlands, pp. 333–337.

Strasser, R.J., Tsimilli-Michael, M., 2001. Stress in plants, from daily rhythm to global changes, detected and quantified by the JIP-test. Chimie Nouvelle (SRC) 75, 3321–3326.

Strasser, R.J., Srivastava, A., Govindjee, 1995. Polyphasic chlorophyll a fluorescence transient in plants and cyanobacteria. Photochem. Photobiol. 61, 32–42.

Strasser, R.J., Srivastava, A., Tsimilli-Michael, M., 2000. The fluorescence transient as a tool to characterize and screen photosynthetic samples. In: Mohanty, P., Yunus, M., Pathre, U. (Eds.), Probing Photosynthesis: Mechanism, Regulation & Adaptation. Taylor & Francis, London, pp. 443–480.

Strehler, B.L., Arnold, W., 1951. Light production by green plants. J. Gen. Physiol. 34, 809–820.

Tsimilli-Michael, M., Krüger, G.H.J., Strasser, R.J., 1996. About the perpetual state changes in plants approaching harmony with their environment. Archs Sci. Genuve 49, 173–203.

Van Gorkom, H.J., Donze, M., 1973. Charge accumulation in the reaction center of photosystem 2. Photochem. Photobiol. 17, 333–342.

Vass, I., Govindjee, 1996. Thermoluminescence from the photosynthetic apparatus. Photosynth. Res. 48, 117–126.

Vesselovskii, V.A., Veselova, T.V., 1990. Plant luminescence, Nauka, Moscow (In Russian).

Vredenberg, W.J., Bulychev, A.A., 2002. Photo-electrochemical control of photosystem II chlorophyll fluorescence in vivo. Bioelectrochemistry 57, 123–128.

Wraight, C.A., Crofts, A.R., 1971. Delayed fluorescence and the high-energy state of chloroplasts. Eur. J. Biochem. 19, 386–397.

Zaharieva, I., Taneva, St.G., Goltsev, V.N., 1999. Effect of PS II antennae size on the induction kinetics of prompt and delayed chlorophyll fluorescence. Bulg. J. Plant Physiol. 25, 17–30.

Zaharieva, I., Taneva, St.G., Goltsev, V.N., 2001. Effect of temperature on the luminescent characteristics in leaves of *Arabidopsis* mutants with decreased unsaturation of the membrane lipids. Bulg. J. Plant Physiol. 27, 3–18.

Zaharieva, I., Goltsev, V., 2003. Advances on Photosystems II investigation by measurement of delayed chlorophyll fluorescence by a phosphoroscopic method. Photochem. Photobiol. 77, 292–298.

Zankel, K.L., 1971. Rapid delayed luminescence from chloroplasts: kinetic analysis of components; the relationship to the O_2 evolving system. Biochim. Biophys. Acta 245, 373–385.